ELSEVIER

Journal of Nuclear Materials 290–293 (2001) 1088–1092

journal of nuclear materials

www.elsevier.nl/locate/jnucmat

Lateral deflection of the SOL plasma during a giant ELM

I.S. Landman [a,*], H. Wuerz [b]

[a] Troitsk Institute for Innovation and Fusion Research, 142092 Troitsk, Russian Federation
[b] Forschungszentrum Karlsruhe, P.O. Box 3640, 76021 Karlsruhe, Germany

Abstract

In recent H-mode experiments at JET with giant ELMs a lateral deflection of hot tokamak plasma striking the divertor plate has been observed. This deflection can effect the divertor erosion caused by the hot plasma irradiation. Based on the MHD model for the vapor shield plasma and the hot plasma, the Seebeck effect is analyzed for explanation of the deflection. At $t = -\infty$ both plasmas are at rest and separated by a boundary parallel to the target. The interaction between plasmas develops gradually ('adiabatically') as $\exp(t/t_0)$ with $t_0 \sim 10^2$ μs the ELM duration time. At inclined impact of the magnetized hot plasma a toroidal current develops in the interaction zone of the plasmas. The $\mathbf{J} \times \mathbf{B}$ force accelerates the interacting plasmas in the lateral direction. The cold plasma motion essentially compensates the current. The magnitude of the hot plasma deflection is comparable to the observed one.

Keywords: Divertor target; $\mathbf{E} \times \mathbf{B}$ drift; ELM; H-mode; JET

1. Introduction

To achieve better plasma confinement the H-mode of operation is used in tokamaks, in which edge localized modes (ELMs) develop [1]. During an ELM, the expelled hot plasma is lost to the scrape-off layer (SOL) and is guided to the divertor along the magnetic field lines (see Fig. 1). This can result in rather serious divertor damage. In recent H-mode experiments at JET with giant ELMs, a lateral deflection of both separatrix strike points has been observed [2]. During the initial stage of ELMs, the separation of the strike points increased between 20 and 36 cm. This deflection can effect the divertor erosion because of enlarging the irradiated area.

From the experiments and their interpretation it is unclear which physical mechanism produces the lateral deflection. For ELMs of duration of 10^2 μs and target heat loads in the 10 GW/m^2 range the eroded material (carbon or beryllium) forms a vapor layer which shields the target [3]. The numerical simulation of the hot plasma target interaction has to include the influence of the lateral deflection of the vapor shield, because of its influence on the shielding efficiency. Up to now two models handling the deflection mechanisms are available [4,5]. Both models include the vapor shield and are based on the thermoelectric effect, which depends on the inclination angle α of the magnetic field to the target. The presented approach improves the model of Landman [5] aiming to explain the mentioned experimental results.

2. Main assumptions and equations

Initially the hot plasma heats the unshielded wall. After some time vaporization starts and the vapor shield develops. The thermoelectric effect accompanies this process from the very beginning, but the starting phase is not taken into account. The analysis starts from two toroidal plasmas initially being at rest (see Fig. 2). For the lateral (y) and toroidal (z) coordinates symmetry is assumed ($\partial/\partial y = 0, \quad \partial/\partial z = 0$). The plasmas have the sizes $a_x, \quad a_y$ and a_z with $a_x = L_c$ for the cold plasma and $a_x = L_h$ for the hot plasma. The

* Corresponding author. Tel.: +49-07247 824696; fax: +49-07247 824874.
E-mail address: landman@ihm.fzk.de (I.S. Landman).

0022-3115/01/$ - see front matter
PII: S0022-3115(00)00548-1

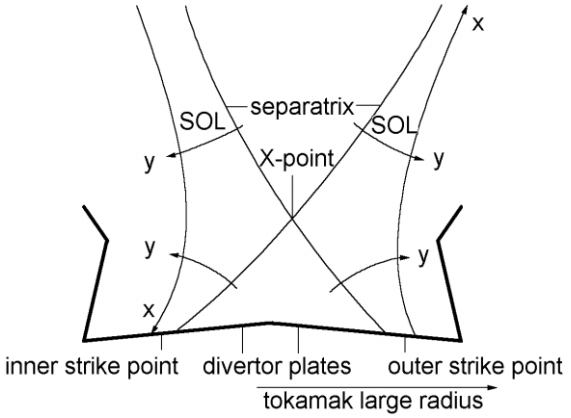

Fig. 1. The divertor and the geometry of the SOL schematically. The strike points of the SOL plasma are located at the divertor plates. The toroidal coordinate z (not shown) is orthogonal to x- and y-axes. The lines of poloidal magnetic field indicate the x-axis.

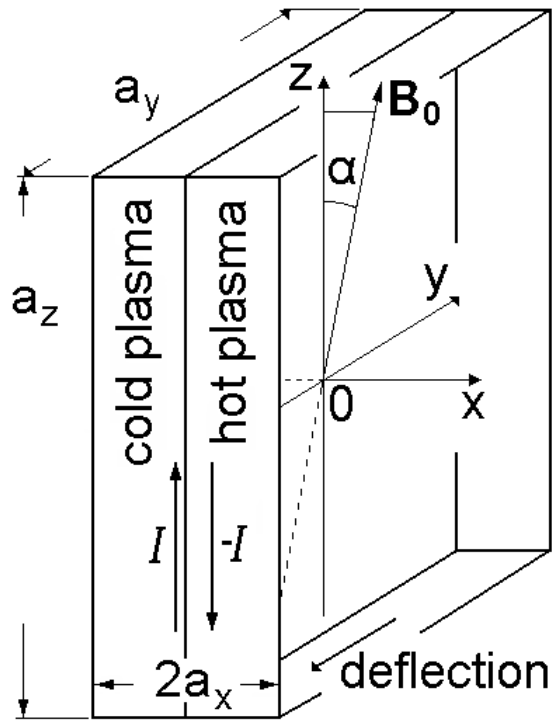

Fig. 2. Positions of the plasmas schematically. a_x, a_y and a_z are the plasma sizes with a_x shown in the figure to be equal for both plasmas. Compensating toroidal currents I and $-I$ are developing in the hot–cold plasma interface. The lateral deflection develops in y-direction.

components of the initial magnetic field are given as $\mathbf{B}_0 = (B_x, 0, B_z)$ with $B_x = B_0 \sin\alpha$, $B_z = B_0 \cos\alpha$. Electric currents in x- and y-directions are assumed to vanish thus it remains only an eddy current I in toroidal direction.

A large difference is assumed to be between the hot and the cold plasma temperatures ($T_h \gg T_c$). With this condition, the stopping length λ_e of the hot electrons in the cold plasma is much larger than that of the hot ions. The hot electrons propagate into the cold plasma or penetrate into the target getting absorbed there. The hot ions are assumed to be stopped at the boundary between the plasmas. Thus in the cold plasma an electron flux appears, which compensates the flux of the hot electrons and produces a toroidal current of density J_z. This current produces the z-component E_z of the electric field $\mathbf{E}$ and a perturbation B_y of $\mathbf{B}_0$ (below it is shown that B_y is small compared to B_0). The fields E_z and B_y obey Maxwell's equations

$$\frac{\partial B_y}{\partial x} = \frac{4\pi}{c} J_z, \quad \frac{\partial B_y}{\partial t} = c\frac{\partial E_z}{\partial x}, \quad B_y|_{\text{init}} = 0. \tag{1}$$

The x-component of $\mathbf{E}$ is given as $E_x = -\partial\phi/\partial x$ with ϕ the electric potential obtained from the quasineutrality equation $n_e = n_i = n_h$ for the hot plasma and $n_{ce} = Zn_{ci}$ for the cold plasma with Z the mean charge state and n the particle densities. n_h is small compared to n_{ci} and n_{ce}. The pressure balance is given as $(n_{ci} + n_{ce})T_c \approx 2n_h T_h$.

The final magnitude of the deflection depends significantly on the evolution of the plasma interaction, which in turn depends on the hot electron current J_{he} in the cold plasma. The regime adequately fitting to the experiment assumes a gradually ('adiabatically') switching on of J_{he} according to $\exp(t/t_0)$ with t_0 the time duration of the ELM. The initial time moment corresponds to $t = -\infty$ and the final one to $t = 0$.

The density n_{he} of the hot electrons in the cold plasma and the current J_{he} are obtained by use of the Boltzmann distribution according to

$$n_{he} = \frac{n_h}{2} \exp\left(-\frac{|x|}{\lambda_e \sin\alpha} - \frac{U(x)}{T_h} \right),$$
$$J_{he} = \frac{e v_{The} n_{he}}{\sqrt{\pi}} \exp\left(\frac{t}{t_0} \right) \tag{2}$$

with $v_{The} = (2T_h/m_e)^{1/2}$ the hot electron thermal velocity. The stopping effect is provided by the exponential factor including λ_e. The potential energy $U(x)$ consists of the sheath potential barrier $\phi_0 \approx T_h/e$ between the plasmas and the 'effective potential' φ according to

$$U(x) = e\phi_0 - e\varphi(x) \quad \text{with} \quad \varphi(x) = \int_x^0 \frac{\mathbf{EB}}{B_0} \frac{\mathrm{d}x}{\sin\alpha}. \tag{3}$$

The lateral plasma motion (in y-direction) is analyzed for both plasmas with the MHD approach. The Euler equation writes as

$$\rho \frac{\partial V_y}{\partial t} = \frac{B_x J_z}{c}, \quad V_y|_{\text{init}} = 0, \tag{4}$$

with V_y the ion velocity and $\rho = \rho_c$ or $\rho = \rho_h$ the mass density. The wall stops the plasma motion, therefore the boundary condition $V_y = 0$ is valid at $x = -L_c$. Another boundary is assumed to simulate the middle plane of the SOL in relation to which the lateral deflection is symmetrical. Thus $\partial V_y/\partial x = 0$ is valid at $x = L_h$.

The whole current is split into the hot and cold electron currents according to

$$J_{hex} + J_{cex} = 0, \quad J_{hey} + J_{cey} = 0, \quad J_{hez} + J_{cez} = J_z \tag{5}$$

with $J_{hex} = J_{he}\sin\alpha$, $J_{hey} = 0$, $J_{hez} = J_{he}\cos\alpha$ and $\mathbf{J}_{ce}$ found from the Ohm's law as

$$\mathbf{J} = \sigma\left(\mathbf{E} + \frac{1}{c}\mathbf{V}_e \times \mathbf{B}\right) \tag{6}$$

with σ the conductivity and $\mathbf{V}_e$ the velocity of cold electrons. In the hot plasma Ohm's law is also applied assuming $\sigma = \infty$.

3. Results of the model

A detailed description of how to solve the system of equations Eqs. (1)–(6) is given elsewhere [6]. The currents J_z and J_{he} are eliminated from the system resulting in an equation for the potential ϕ, the solution of which at small B_y values is obtained as

$$\phi(x) \approx -\frac{T_h}{e}\ln\left(1 + K\left(1 - \exp\left(\frac{sx}{L_h}\right)\right)\right) \tag{7}$$

with the dimensionless parameters

$$K = \frac{e^2\lambda_e \upsilon_{The} n_h \exp(-e\phi_0/T_h)}{2\sqrt{\pi}\sigma T_h}, \quad s = \frac{L_h}{\lambda_e \sin\alpha}. \tag{8}$$

From Ohm's law the equation for B_y is obtained according to

$$\frac{\partial B_y}{\partial t} - B_x\frac{\partial V_y}{\partial x} = \begin{bmatrix} \frac{\partial}{\partial x}\left(\frac{c^2}{4\pi\sigma}\frac{\partial B_y}{\partial x} - \frac{c}{2}\sin 2\alpha \frac{\partial\phi}{\partial x}\exp\left(\frac{t}{t_0}\right)\right), & x < 0 \\ 0, & x > 0 \end{bmatrix}. \tag{9}$$

From Eq. (4) the boundary conditions $\partial B_y/\partial x|_{x=-L_c} = 0$ and $B_y|_{x=L_h} = 0$ are obtained. Eq. (9) requires also the fitting at $x = 0$, which is obtained integrating Eqs. (4) and (9) over a small interval across the boundary thus guaranteeing the continuity of B_y and E_z.

Eqs. (1), (4) and (9) are linear. Due to this an analytical solution is obtained as

$$V_y \approx V_A\frac{\mu a K e^{t/t_0}}{s} \times\left(\frac{e^{sx/L_h}\theta(-x)}{1 + K(1 - e^{sx/L_h})} - \frac{e^{-sl_c}}{1 + K(1 - e^{-sl_c})}\right) \tag{10}$$

with V_A the Alfven velocity and μ, a and l_c the dimensionless parameters given as

$$V_A = \frac{B_0}{\sqrt{4\pi\rho_h}}, \quad \mu = \frac{cT_h t_0\cot\alpha}{eB_0\lambda_e^2}, \quad a = \frac{L_h}{t_0 V_A\sin\alpha}, \quad l_c = \frac{L_c}{L_h}. \tag{11}$$

The lateral deflection is given as $\Delta_y = t_0 V_y$. The parameter K is reversely proportional to the conductivity σ of the cold plasma. Thus according to Eq. (10) if the cold plasma would be a perfect conductor, the deflection would not occur because $\Delta_y \to 0$ at $\sigma \to \infty$.

The magnitude of B_y at the separation boundary is obtained as

$$B_y(t,0) \approx B_0\mu\frac{a^2}{s^2}\exp\left(\frac{t}{t_0}\right)\frac{eL_h}{T_h}\left.\frac{\partial\phi}{\partial x}\right|_{x=-L_c}. \tag{12}$$

In order to estimate the value of the deflection some typical physical parameters are chosen. Unfortunately up to now the SOL plasma temperature T_h and the density n_h have not been measured in ELMs. Nevertheless, it is assumed that n_h is of the order of 3×10^{13} cm^{-3} and T_h of 3 keV. From the calculations of [3] the temperature of the cold plasma T_c is assumed to be 30 eV. A deuterium hot plasma and a graphite plate in the inclined magnetic field with $B_0 = 5$ T and $\alpha = 0.1$ rad are applied. In case of graphite, $Z = 5$ is a typical value for the charge state.

For these conditions and with $L_h = 1$ m, $\rho_c = 12 m_p n_{ci}$ and $\rho_h = 2 m_p n_h$, and using the pressure balance equation, the parameters K, s, μ, and a are obtained as

$$K = 1.2, \quad s = 1.4, \quad \mu = 1.1\times10^{-2}, \quad a = 1/140. \tag{13}$$

In these estimations the conductivity is expressed as $\sigma = e^2 n_{ce}\tau_{ce}/m_e \approx 3\times10^{14}$ s^{-1}. The electron–ion collision time in the cold plasma is given as $\tau_{ce} = 3.5\times10^4 (T_c)^{3/2}/(Z n_{ce}) \approx 2\times10^{-10}$ s with T_c in electronvolts. The stopping length is given as $\lambda_e = \upsilon_{The}\tau_s \approx 6$ m with $\upsilon_{The} \approx 3\times10^9$ cm/s and $\tau_s = \tau_{ce}(T_h/T_c)^{3/2} \approx 2\times10^{-7}$ s.

From Eq. (10) follows that maximum deflection of the hot plasma is obtained for $L_c \ll \lambda_e\sin\alpha$. The hot electrons mainly reach the target and the hot plasma deflection Δ_h is larger than that of the cold plasma Δ_c. The relation of the deflection is given as $\Delta_c/\Delta_h \approx (K+1)L_c/(\lambda_e\sin\alpha)$. For typical values of physical parameters, Δ_h is obtained as $\Delta_h \approx 7$ cm. The behavior of Δ_h at $L_c \ll \lambda_e\sin\alpha$ is given as

$$\Delta_h\ [\text{cm}] \approx \frac{0.7Z}{5\tan\alpha}\exp\left(1 - \frac{e\phi_0}{T_h}\right)\frac{t_0}{10^2\mu\text{s}}\left(\frac{30\text{ eV}}{T_c}\right)^{3/2} \times\frac{5\text{T}}{B_0}\left(\frac{T_h}{3\text{ keV}}\right)^{1/2}\frac{n_h}{3\times10^{13}\text{ cm}^{-3}}. \tag{14}$$

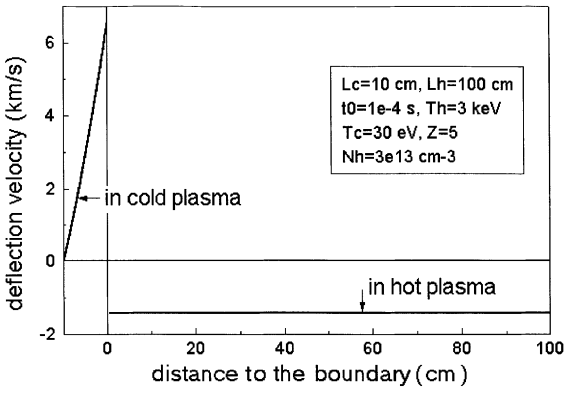

Fig. 3. The deflection velocity after 100 μs.

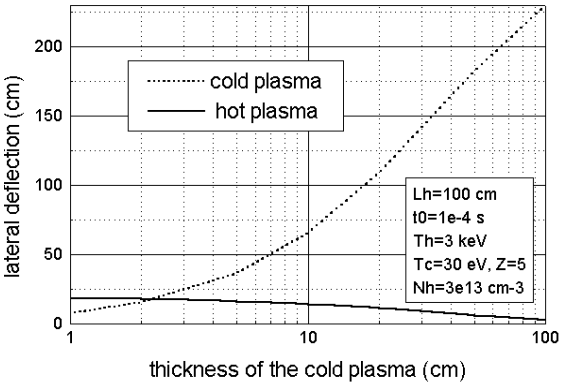

Fig. 4. The deflection of the plasmas after 100 μs as a function of the cold plasma thickness.

A typical behavior of the deflection velocity is shown in Fig. 3. The deflections of the hot and cold plasma in a wide region of the parameter L_c are shown in Fig. 4.

4. Discussion of the results

In order to provide the linear character of the analyzed problem the assumption that B_y is small was used. For the adiabatic development of the plasma interaction B_y is obtained from Eq. (12). At the final time moment and for a the small thickness of the cold plasma B_y gets about 0.02 G. Despite of such a small value of the induced magnetic field, the lateral deflection of the hot plasma being of the order of the experimentally measured values occurs only due to the non-zero B_y. The small contribution of the vortex electric field to φ makes the effective potential equal to the usual electric potential with a good accuracy.

The observation that the deflection occurs only due to the inclination of the magnetic field is met in the presented model because according to Eq. (14) the larger the inclination (the smaller α) the larger the deflection.

The assumption of an adiabatic increase of the interaction intensity in which the characteristic time of the switching on of the plasmas interaction is of the order of t_0 seems to be reasonable. In this case , the amplitudes of the high frequency parasitic modes become negligibly small if t_0 is much larger than their oscillation period. The deflection velocity at each time moment depends only on the intensity of the current generation. In the opposite case of a sudden start of the interaction the induced self-consistent electromagnetic field propagates with the Alfven velocity along the magnetic field lines into the hot plasma as a pulse. A similar wave propagates in the cold plasma. In reality the wave front reaches the boundary of the hot plasma in a time $L_h/(V_A \sin|\alpha|)$ being much smaller than t_0. Due to the reflection from the boundary, plasma modes of rather high frequencies and amplitudes would occur. For the above-mentioned typical parameters, the Alfven velocity is obtained as $V_A \approx 10^9$ cm/s. Using the value $L_h = 1$ m the relation of t_0 to the time of the mode propagation through the plasmas is estimated as $a^{-1} \sim 10^2$. Thus the mode frequencies are of the order of $1/(t_0 a)$, which does not relate with the characteristic time t_0 of the problem under consideration. Similar remarks concern the cold plasma.

According to Eq. (10), the lateral velocity of the hot plasma is proportional to the factor $[\exp -L_c/(\lambda_e \sin\alpha)]$. Thus, when increasing the thickness L_c of the vapor shield the lateral velocity decreases. According to Eq. (14), the hot plasma deflection velocity is proportional to $(T_c)^{3/2}$ and thus should be larger at the initial stage of an ELM. Hence the experimental observation that the strike points mainly move before arrival of the power flux pulse correlates well with the model.

5. Conclusion

SOL plasma deflection may play a significant role in the problem of hot plasma–solid wall interaction because the exposition area of the hot plasma is increased and because of the development of an additional mechanism of cold plasma removal from the exposed area. Due to this the target screening may get less effective, thus causing enhanced wall erosion despite the decrease of the average target heat load. A first simulation of the plasma–target interaction with a given lateral velocity of the hot plasma showed significant decrease of erosion. But for drawing final conclusions a consistent simulation of vapor shield and deflection is necessary.

Despite rather significant mathematical simplifications of the plasma–target interaction, which were necessary for the development of the analytical model for the deflection effect, the approach seems fruitful. The quantitative agreement and the qualitative similarity of the theoretical and the experimental results demonstrate that the physical picture used is relevant for the real deflection phenomenon. The still rather artificial one-dimensional model considered in this work may be useful for the development of a more adequate one- and two-dimensional numerical simulation of the plasma target interaction with accounting for the lateral deflection of both the hot SOL plasma and the vapor shield layer.

References

[1] M. Keilhacker, M.L. Watkins, JET Team, J. Nucl. Mater. 266–269 (1999) 1.
[2] J.A. Lingertat et al., J. Nucl. Mater. 241–243 (1997) 402.
[3] H. Wuerz et al., Nucl. Instrum. and Meth. A 415 (1998) 543.
[4] L.L. Lengyel et al., Nucl. Fus. 37 (1997) 1245.
[5] I. Landman, H. Würz, in: 24th EPS, Vol. 21A, Part IV, Berchtesgaden, 1997, p. 1821.
[6] I.S. Landman, H. Wuerz, Report FZKA 6469, Forschungszentrum Karlsruhe, 2000.